

# Artifact Reduction in T1 $\rho$ -weighted Images: An Algorithm to Predict Artifact Reduction in Pulse Clusters

D. J. Wallman<sup>1</sup>, W. R. Witschey<sup>2</sup>, A. Borthakur<sup>1</sup>, M. A. Elliott<sup>1</sup>, S. Niyogi<sup>3</sup>, C. Wang<sup>3</sup>, and R. Reddy<sup>1</sup>

<sup>1</sup>Radiology, University of Pennsylvania, Philadelphia, PA, United States, <sup>2</sup>Biochemistry & Molecular Biophysics, University of Pennsylvania, Philadelphia, PA, United States, <sup>3</sup>Bioengineering, University of Pennsylvania, Philadelphia, PA

**Introduction:** T1 $\rho$ -weighted imaging generates useful clinical contrast unlike standard T2-weighted imaging and is sensitive to early osteoarthritis (2), metabolic H<sub>2</sub><sup>17</sup>O (3), cerebral ischemia (1) and breast tumor growth. (4) In T1 $\rho$ -weighted imaging, magnetization relaxes under the influence of a low frequency continuous wave RF pulse; however, spin-lock pulse clusters implementing either integrated spin echo (5) or rotary echo (6) methods are more effective in compensating for inhomogeneous B<sub>0</sub> and B<sub>1</sub> fields, respectively. To explore other spin locking pulse clusters with insensitivity to field gradients, we simulated 320 variations of the spin locking experiment by alternating the pulse cluster composition and phase of each of the RF pulses using the Bloch equations. Due to time-constraints implementing and testing sequences, we instead identify working sequences *a priori* and test them. We confirmed that two pulse sequences for T1 $\rho$  and T2 $\rho$  are artifact free at all  $\omega_1$  field strengths and implement these sequences to image agarose phantoms and *in vivo* human brain.

**Methods:** Using the Bloch equations and a generalized spin-lock pulse sequence (Fig. 1), a permutation of possible spin-lock pulse clusters was created consisting of rotary echo or spin echo implementations with arbitrary pulse phase composition for pulses 2-5. Additional feasible sequences were identified by rotating the phase of all pulses 90°, but provide redundant information. The simulation algorithm is shown diagrammatically and resulted in 320 different spin-lock sequences (Fig. 2). Volunteers were recruited to the study and scanned following a pre-approved protocol by the IRB of the University of Pennsylvania. Imaging was performed using variations of a T1 $\rho$ -prepared fast spin echo sequence with the following imaging parameters (TE<sub>eff</sub>/TR = 13/2500 ms, 128x128 image matrix, FOV = 23 cm<sup>2</sup>, slice thickness = 4 mm, ETL = 7, BW = 130 Hz/pixel. Agarose (3% w/v, 200 mM <sup>23</sup>Na) imaging was performed using a similar protocol (FOV = 15 cm<sup>2</sup>). B<sub>0</sub> and B<sub>1</sub> field maps were collected and processed using a protocol described elsewhere (Abstract #4900). Statistical correlation between simulated and experimental images was performed in MatLab 7.0. Experimental image intensity was normalized to the 98<sup>th</sup> quantile and plotted pixel by pixel against simulated images (intensity = 0-1). A linear regression was calculated and statistical significance was determined with a t-test.

**Results:** The simulation identified two working sequences (# 201 & 230) in addition to a known sequence cluster (Abstract #4900) for field insensitive spin locking among many alternatives (i.e. #44) (Fig. 3). Because the simulation could not distinguish between T1 $\rho$  or T2 $\rho$  pulse cluster implementations, #201 is a sequence for T2 $\rho$ -weighted imaging and demonstrates insensitivity to field variations in both agarose phantoms and in *in vivo* human brain images (Fig. 3). The second (#230) is a T1 $\rho$ -weighted imaging pulse cluster that is also insensitive to field inhomogeneities. Simulated images are shown alongside T1 $\rho$ -weighted and T2 $\rho$ -weighted images of agarose and *in vivo* Human Brain (Fig 3). In sequence 201 and 230, we can see that the artifacts are removed almost completely in both the simulation agarose image and the real agarose image. The identified sequences were also used to obtain images in *in vivo* human brain. There is a linear correlation between normalized experimentally acquired images and the simulated images from B<sub>0</sub> and B<sub>1</sub> maps for both brain and agarose acquisitions (p < 0.001).

**References:** Grohn OH, Lukkariinen JA, Silvennoinen MJ, Pitkanen A, van Zijl PC, Kauppinen RA. Magn Reson Med 1999;42(2):268-276. 2. Regatte RR, et al. Acad Radiol 2004;11(7):741-749. 3. Taylor DR, et al. Magn Reson Med 2003;49(1):1-6. 4. Santyr GE, et al. Magn Reson Med 1989;12(1):25-37. 5. Avison M, et al. A Composite Spin-Lock Pulse for deltaB0 + B1 Insensitive T1rho Measurement. 2006; ISMRM Seattle, WA 6. Charagundla SR, et al. JMR. 2003;162(1):113-121.

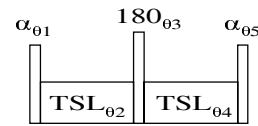


Fig. 1: A generalized spin locking pulse cluster for T1 $\rho$ -weighted imaging. The generalized cluster consists of excitation (phase = 01), spin locking (02, 04), spin echo (03) and storage (05) RF pulses followed by fast spin echo acquisition.

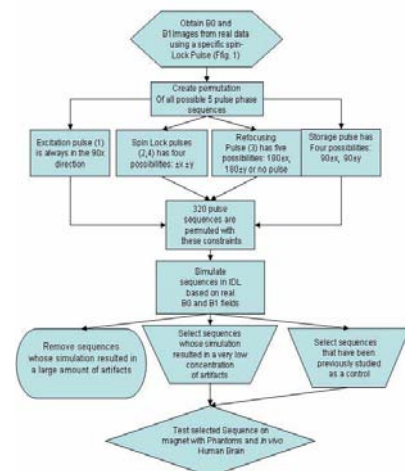


Fig. 2: A computer algorithm to determine *a priori* T1 $\rho$ -weighted pulse clusters insensitive to B<sub>1</sub> and B<sub>0</sub> field gradients. The algorithm calculates the resultant magnetization at the end of a spin locking pulse cluster from only B<sub>0</sub> and B<sub>1</sub> fieldmaps and can be generalized to any pulse sequence.

|                | B <sub>0</sub> Field Map | B <sub>1</sub> Field Map | Simulation Agarose Image   | Exp. Agarose | <i>In Vivo</i> Human Brain |
|----------------|--------------------------|--------------------------|--|--------------|----------------------------|
| Sequence Names |                          |                          |  |              |                            |
| 044            |                          |                          | 90x TSL <sub>y</sub><br>TSL <sub>x</sub> 90x<br>Note: no 180 pulse         |              |                            |
| 201            |                          |                          | 90x TSL <sub>x</sub><br>180x TSL <sub>x</sub><br>90x<br>T2 $\rho$ sequence |              |                            |
| 230            |                          |                          | 90x TSL <sub>y</sub><br>180x TSL <sub>y</sub><br>90x<br>T1 $\rho$ sequence |              |                            |

Fig. 3: Experimental agarose and human brain images shown alongside simulated images in inhomogeneous B<sub>0</sub> and B<sub>1</sub> fields. Sequence variant #44 is an example of a non-ideal sequence for spin locking, while #201 and #230 demonstrate field insensitive T2 $\rho$ - and T1 $\rho$ -weighted imaging variants.